

# Interfacial Interaction of Nickel with Liquid Pb-free Sn-Bi-In-Zn-Sb Soldering Alloys

K. Barmak, D.C. Berry, Carnegie Mellon University, Pittsburgh, PA 15213, USA

V.R. Sidorko, A.V. Samelyuk, V.I. Dybkov, Institute for Problems of Materials Science, 03180 Kyiv, Ukraine

Keywords: Nickel, Liquid Pb-free Solders, Dissolution kinetics, Ni<sub>3</sub>Sn<sub>4</sub> layer growth rate, Joint tensile strength

## Abstract

Dissolution kinetics of nickel in liquid 87.5% Sn-7.5% Bi-3% In-1% Zn-1% Sb and 80% Sn-15% Bi-3% In-1% Zn-1% Sb soldering alloys and phase formation at the Ni-solder interface have been investigated at 250-450°C. The temperature dependence of the nickel solubility in soldering alloys was found to obey a relation of the Arrhenius type  $c_s = 4.94 \times 10^2 \exp(-39500/RT)$  % for the former alloy and  $c_s = 4.19 \times 10^2 \exp(-40200/RT)$  % for the latter, where  $R$  is in  $\text{J mol}^{-1} \text{K}^{-1}$  and  $T$  in K. The dissolution rate constants are rather close for these alloys and vary in the range  $(1-9) \times 10^{-5} \text{ m s}^{-1}$  at disc rotational speeds of 6.45 to 82.4  $\text{rad s}^{-1}$ . With both alloys, the Ni<sub>3</sub>Sn<sub>4</sub> intermetallic layer is formed at the interface of nickel and the saturated or undersaturated melt at holding times up to 2400 s. A simple mathematical equation is proposed to evaluate the Ni<sub>3</sub>Sn<sub>4</sub> layer thickness in the case of undersaturated melts. The tensile strength of the Ni-to-alloy joints is 94-102 MPa.

## Introduction

Since lead is a toxic metal, conventional Sn-Pb solders are gradually being replaced with Sn-based soldering alloys containing additions of other metals. Most frequently employed additives are Ag, Cu, Bi, In, Zn and Sb [1-10]. To avoid the excessive loss of solid metals in contact with soldering alloys during soldering and to prevent the formation of too thick intermetallic layers at the metal-solder interface, data on (i) metal dissolution rates in molten solders and (ii) interfacial phase formation are needed. In this work, the results on the interfacial interaction of solid nickel with liquid 87.5% Sn-7.5% Bi-3% In-1% Zn-1% Sb and 80% Sn-15% Bi-3% In-1% Zn-1% Sb soldering alloys at 250-450°C are reported. According to binary phase diagrams [11], all four additives lower the melting-point temperature of tin. To avoid undesirable phase transformations, indium, zinc and antimony were taken in the amounts, not exceeding their solid-state solubility limits in tin. These elements are known to improve service characteristics of Sn-based solders [12].

## Experimental Procedure

Tin (99.93% Sn), bismuth (99.999% Bi), indium (99.999% In) and antimony (99.91% Sb) slabs, zinc granules (99.94% Zn) and electrolytic-grade nickel plates (99.98% Ni) were used for the investigation.

The process of dissolution of nickel in liquid solders and that of growth of intermetallic layers under conditions of their simultaneous dissolution in the liquid were studied by the rotating disc technique using a rapid-quenching device [13]. A flux was used both to pre-heat the solid specimen to the experimental temperature and to protect the melt from oxidation by atmospheric air. Before the experiment, the solid nickel specimen,  $11.28 \pm 0.02$  mm in diameter ( $1 \text{ cm}^2$  area) and 5-6 mm high, was pressed into a graphite tube to protect its lateral surface from the melt. At the end of the run the nickel specimen was rapidly cooled down in a water bath. Its mass loss during dissolution in the melt was determined by weighing. Alloys obtained after the runs were analyzed chemically to determine their Ni content. Ni content was also found by electron probe microanalysis. Three values were then averaged and used in further calculations.

To investigate the growth process of intermetallic-compound layers from saturated melts, experiments were carried out in a steel thermostat. Polished nickel plates,  $14 \times 5 \times 3 \text{ mm}^3$ , were mounted into graphite crucibles. The crucibles were placed in the thermostat at a required temperature. These were then filled with the flux from a moveable electric-resistance furnace, kept at the same temperature. After the temperature in the thermostat had equilibrated, the crucibles were filled with the metallic melt, previously saturated with nickel, from another moveable electric-resistance furnace, also kept at the required temperature. Nickel was allowed to react with the melt during a predetermined period of time in the 300-1800 s range. Then, the graphite crucibles with their contents were withdrawn from the thermostat and rapidly cooled down in water. Bimetallic specimens obtained were cut into two parts, normal to the long side of a nickel plate. The Ni-solder cross-sections were prepared and examined with the use of metallography, X-ray diffraction and electron probe microanalysis.

## Results and Discussion

### Dissolution Kinetics

The dissolution process of a solid metal in a liquid solder is described by the Nernst-Shchukarev equation [13]

$$\ln \frac{c_s}{c_s - c} = k \frac{st}{v} \quad (1)$$

where  $c$  is the instantaneous concentration of the dissolved metal in the liquid phase,  $c_s$  is the solubility at a given temperature,  $k$  is the dissolution rate constant,  $s$  is the surface area of the solid,  $v$  is the liquid volume, and  $t$  is the time.

Equation 1 indicates that the process of dissolution of a solid in a liquid is characterized by two quantities, namely, the solubility or saturation concentration,  $c_s$ , and the dissolution rate constant,  $k$ . At the constant pressure the saturation concentration only depends upon temperature. The dissolution rate constant is in addition dependent upon the hydrodynamic conditions of flow of the liquid.

### *Solubility of Ni in Liquid Solders*

From Eq. 1, the concentration of the dissolved substance in the liquid is seen to increase with passing time and eventually to reach its limiting value,  $c_s$ , as was the case for the nickel

content in 87.5% Sn-7.5% Bi-3% In-1% Zn-1% Sb and 80% Sn-15% Bi-3% In-1% Zn-1% Sb soldering alloys (Fig. 1).

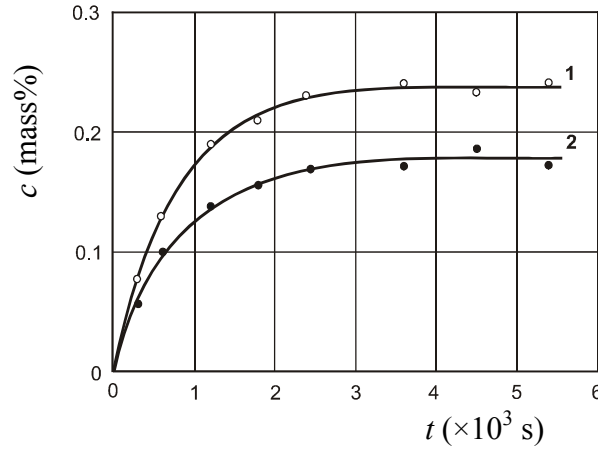


Figure 1 Nickel contents, dissolved into soldering alloys, are plotted against time to determine the solubility (saturation concentration),  $c_s$ . Rotational speed  $\omega = 54.0 \text{ rad s}^{-1}$ ,  $s/v = 27.5 \text{ m}^{-1}$ .  
1, 87.5% Sn-7.5% Bi-3% In-1% Zn-1% Sb alloy; 2, 80% Sn-15% Bi-3% In-1% Zn-1% Sb alloy

The temperature dependence of the solubility of nickel in the solders was found to obey a relation of the Arrhenius type  $c_s = A \exp(-E/RT)$ , where  $A$  is the frequency factor,  $E$  is the activation energy (enthalpy of dissolution),  $R$  is the gas constant and  $T$  is the absolute temperature. Application of the least-squares fit method yielded the following equations:  
 $c_s = 4.94 \times 10^2 \exp(-39500/RT)$  % for a 87.5% Sn-7.5% Bi-3% In-1% Zn-1% Sb alloy,  
 $c_s = 4.19 \times 10^2 \exp(-40200/RT)$  % for a 80% Sn-15% Bi-3% In-1% Zn-1% Sb alloy,  
 where  $R$  is in  $\text{J mol}^{-1} \text{ K}^{-1}$  ( $8.314 \text{ J mol}^{-1} \text{ K}^{-1}$ ) and  $T$  in K.

Note that relatively small amounts of additives produce a very considerable effect on the solubility of nickel in Sn-base soldering alloys. The temperature dependence of the nickel solubility in pure tin at 300-700 °C is reported to obey the equation [14]  
 $c_s = 5.34 \times 10^2 \exp(-36900/RT)$  %.

Comparison of the solubility values calculated from these three temperature dependences is provided in Table 1. Twenty percent of additives (Bi, In, Zn and Sb) are seen to produce more than a two-fold decrease in nickel solubility values. Such a large drop could not be expected judging from the solubility values in binary systems of nickel with the main alloy constituents tin and bismuth. For example, at 350 °C  $c_s$  is 0.43% Ni for tin [14] and 0.39% Ni for bismuth [15]. In view of their relatively low content in the alloys, the influence of indium, zinc and antimony can hardly be significant. Note that for a similar alloy containing 51% Bi, 42% Sn, 5% In and 2% Zn the nickel solubility at 350 °C is much lower, namely, 0.015% [15]. These data provide evidence that the solubility values decrease as the alloy composition approaches from both sides to the composition of the binary eutectic Bi-Sn (57% Bi and 43% Sn [11]).

### **Dissolution Rate Constants of Ni in Liquid Solders**

Besides the solubility,  $c_s$ , another main characteristic of the dissolution process of a solid metal in a liquid solder is the dissolution rate constant,  $k$ . To obtain an accurate measure of this

constant, the initials parts of the dissolution curves such as those shown in Fig. 1 were investigated in detail at an angular disc rotational speed of  $24.0 \text{ rad s}^{-1}$ . The linearity of a plot of  $\ln [c_s/(c_s - c)]$  against  $st/v$  in Fig. 2 provides evidence for the validity of Eq. 1, which can thus be used to determine accurate values of the dissolution rate constant.

**Table 1 Solubility,  $c_s$ , dissolution rate constant,  $k$ , at disc rotational speed of  $24.0 \text{ rad s}^{-1}$ , and diffusion coefficients,  $D$ , of nickel in liquid solders**

Temperature (°C)	$c_s$ (%)			$k$ ( $\times 10^{-5} \text{ m s}^{-1}$ )		$D$ ( $\times 10^{-5} \text{ m}^2 \text{ s}^{-1}$ )	
	100% Sn [14]	87.5% Sn...	80% Sn...	87.5% Sn...	80% Sn...	87.5% Sn...	80% Sn...
250	0.11	0.056	0.040	1.3	1.1	0.22	0.16
300	0.23	0.12	0.091	2.7	2.6	0.59	0.56
350	0.43	0.24	0.18	4.6	4.5	1.33	1.28
400	0.73	0.42	0.32	5.4	5.3	1.68	1.63
450	1.15	0.69	0.52	6.2	6.1	2.02	2.02

Experimental values of the dissolution rate constant at a disc rotational speed of  $24.0 \text{ rad s}^{-1}$  are included in Table 1. Dissolution rate constants obtained at  $350 \text{ }^\circ\text{C}$  and other rotational speeds are presented in Table 2. The mean relative error of their determination is  $\pm 8\%$ .

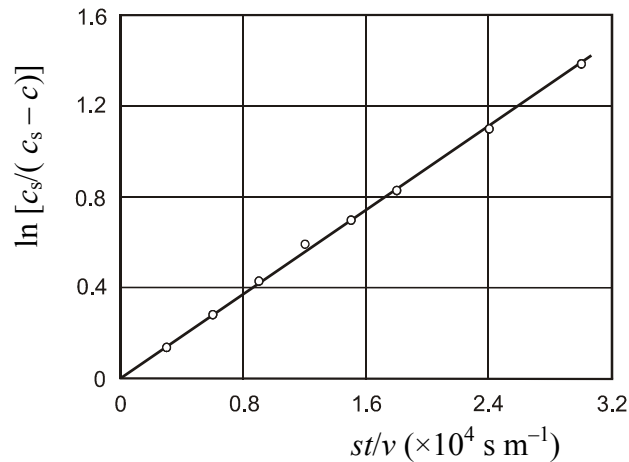


*Figure 2 A plot of  $\ln [c_s/(c_s - c)]$  against  $st/v$  for a liquid 87.5% Sn-7.5% Bi-3% In-1% Zn-1% Sb alloy at a temperature of  $350 \text{ }^\circ\text{C}$ . Disc rotational speed  $\omega = 24.0 \text{ rad s}^{-1}$ ,  $s/v = 10.0 \text{ m}^{-1}$*

Note that, although the solubility values at a given temperature differ considerably, appropriate dissolution rate constants of nickel in these soldering alloys are very close. Their values fall in the range  $(1-10) \times 10^{-5} \text{ m s}^{-1}$ .

**Table 2 Dissolution rate constants,  $k$ , of nickel in liquid solders at 350 °C and disc rotational speeds in the range 6.45-82.4 rad s<sup>-1</sup>**

$\omega$ (rad s <sup>-1</sup> )		6.45	9.00	15.3	24.0	32.7	54.0	82.4
$k$ ( $\times 10^{-5}$ m s <sup>-1</sup> )	87.5% Sn...	2.6	2.9	3.9	4.6	5.8	7.0	9.0
	80% Sn...	2.4	3.1	3.7	4.5	5.2	7.3	8.8

### ***Diffusion Coefficients of Ni in Liquid Solders***

For a rotating disc, the dissolution rate constant,  $k$ , is related to the diffusion coefficient,  $D$ , of the solute atoms into the bulk of the liquid, the melt viscosity,  $\nu$ , and the angular rotational speed,  $\omega$ , through the equations [16, 17]

$$k = 0.62D^{2/3}\nu^{-1/6}\omega^{1/2} \quad (2)$$

$$k = 0.554I^{-1}D^{2/3}\nu^{-1/6}\omega^{1/2} \quad (3)$$

where  $I$  is a function of the Schmidt number,  $Sc$  ( $Sc = \nu/D$ ).

The  $k - \omega^{1/2}$  dependence was found to be linear at  $\omega = 6.45$  to  $82.4$  rad s<sup>-1</sup>, indicative of diffusion-controlled dissolution process. Nickel diffusivities found from Eq. 3 are listed in Table 1. The mean relative error of their determination is  $\pm 12\%$ . Diffusion coefficients of nickel in liquid solders thus obtained are clearly averages for the concentration range  $0 - c_s$ . However, in view of the narrowness of this range, the concentration dependence of the diffusion coefficient may reasonably be expected to be insignificant.

### **Formation of Intermetallic Layers at the Ni-Solder Interface**

Two sets of experiments were carried out to visualize the effect of dissolution on the process of intermetallic compound-layer formation at the interface between nickel and liquid Pb-free solders. In the first set, the solder melt previously saturated with nickel was employed. Therefore, dissolution of the solid nickel in the liquid phase did not occur.

In the second, the melt initially contained no nickel. Hence, the intermetallic layers were formed under conditions of their simultaneous dissolution in the solder melt. In this case, the nickel disc was being rotated during the run at an angular speed of  $24.0$  rad s<sup>-1</sup>.

### **Theoretical Analysis**

#### ***Intermetallic Layer Formation from a Saturated Melt***

The  $A_pB_q$  intermetallic layer growth at the interface between a solid metal  $A$  and a liquid solder  $B$  is a result of counter-diffusion of components  $A$  and  $B$  across its bulk followed by appropriate partial chemical reactions [18]. These reactions yield the increases,  $dx_{B1}$  and  $dx_{A2}$ , in layer thickness during a time,  $dt$  (Fig. 3).

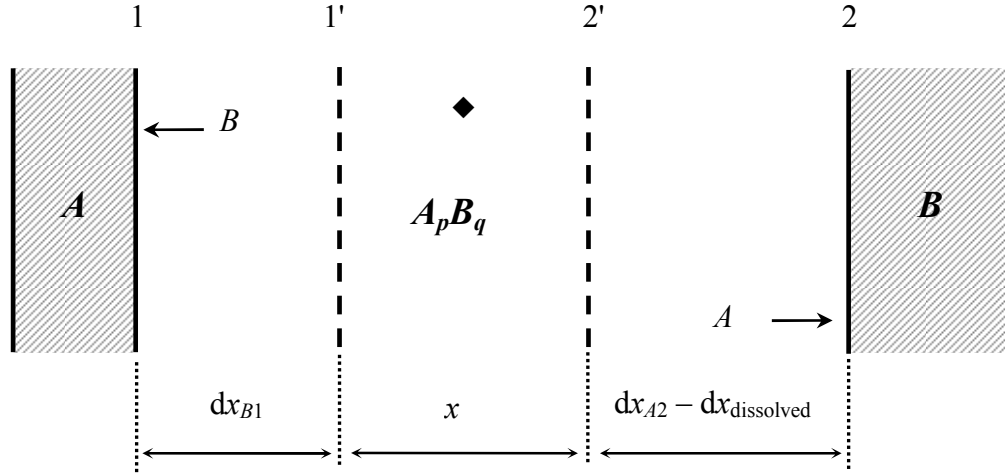


Figure 3 Schematic diagram to illustrate the mechanism of formation of the  $A_p B_q$  intermetallic layer under conditions of its simultaneous dissolution in the solder melt. The changes in layer thickness are measured relative to an inert marker ( $\blacklozenge$ ) located inside the layer

In the case of a liquid solder  $B$  saturated with  $A$ , the layer-growth rate is

$$\left(\frac{dx}{dt}\right)_{\text{growth}} = \frac{k_{0B1}}{1 + \frac{k_{0B1}x}{k_{1B1}}} + \frac{k_{0A2}}{1 + \frac{k_{0A2}x}{k_{1A2}}} \quad (4)$$

where  $k_{0B1}$  and  $k_{0A2}$  are chemical constants, and  $k_{1B1}$  and  $k_{1A2}$  are diffusional constants (reaction-diffusion coefficients). The layer-growth kinetics are initially linear (at  $x$  up to 500-600 nm) and then parabolic ( $x > \sim 1 \mu\text{m}$ ).

### ***Effect of Dissolution in the Solder Melt on the Layer Growth Rate***

As seen in Fig. 3, the net rate of layer formation is the difference between the rates of its growth at interfaces 1 and 2 and dissolution at interface 2. The layer dissolution rate is

$$\left(\frac{dx}{dt}\right)_{\text{dissolution}} = b_t = b_0 \exp(-at) \quad (5)$$

where  $b_0 = c_s k / \rho \varphi$ ,  $a = ks/v$ ,  $\rho$  is the density of the  $A_p B_q$  compound,  $\varphi$  is the content of  $A$  in  $A_p B_q$  in mass fractions.

A mathematical equation describing the growth kinetics of any intermetallic layer  $A_p B_q$  at the  $A$ - $B$  interface under conditions of its simultaneous dissolution in the liquid phase is

$$\left(\frac{dx}{dt}\right) = \frac{k_{0\text{Sn1}}}{1 + \frac{k_{0\text{Sn1}}x}{k_{1\text{Sn1}}}} + \frac{k_{0\text{Ni2}}}{1 + \frac{k_{0\text{Ni2}}x}{k_{1\text{Ni2}}}} - b_0 \exp(-at). \quad (6)$$

Clearly, the layer growth is generally non-parabolic. Moreover, if

$$k_{0B1} + k_{0A2} < b_0 \quad (7)$$

(sum of the rates of chemical reactions at the interfaces is less than the initial rate of dissolution), it is missing from the *A-B* couple.

As seen from Eq. 5, the dissolution rate diminishes exponentially from  $b_0$  to  $b_t$  in the  $0 - t$  time range. Hence, when  $k_{0B1} + k_{0A2} = b_t$ , the  $A_pB_q$  layer occurs at the *A-B* interface after some delay. At large  $t$ ,  $b_t = 0$ , and the layer-growth kinetics become close to parabolic.

Equation 6 cannot be solved precisely. However, its simpler forms can readily be employed in practice to estimate the thickness of any intermetallic layer growing from an undersaturated solder melt.

### ***Growth of the Intermetallic Layer in the Case of a Constant Dissolution Rate***

If the  $A_pB_q$  layer grows under conditions of diffusion control ( $k_{0B1} \gg k_{1B1}/x$ ,  $k_{0A2} \gg k_{1A2}/x$ ), while the dissolution rate is constant and equal to  $b_t$ , Eq. 6 reduces to  $dx/dt = k_1/x - b_t$ , where only one diffusional constant,  $k_1$ , is retained for simplicity. In such a case, the layer thickness tends with increasing time to a limiting value

$$x_{\max} = k_1/b_t \quad (8)$$

that is defined from the condition  $k_1/x - b_t = 0$ .

### **Ni-Solder Transition Zone Microstructures**

With both soldering alloys, a single-phase intermetallic layer consisting of the  $Ni_3Sn_4$  intermetallic compound was found to form from both saturated and undersaturated melts. Micrographs in Fig. 4 visualize the effect of dissolution on the process of formation of the intermetallic layer at the Ni-solder interface. In the case of the undersaturated melt, the rotating disc technique was employed ( $\omega = 24.0 \text{ rad s}^{-1}$ ). Dissolution is seen to produce around a five-fold decrease in layer thickness.

It should be noted that under conditions of strong solder agitation at 250 °C the  $Ni_3Sn_4$  layer is initially missing (up to 600 s) from the Ni-solder couple (Fig. 5). It provides evidence for the validity of Eq. 7.

### **Evaluation of the Intermetallic Layer Thickness in the Case of Undersaturated Melts**

To estimate the effect of dissolution on the layer-growth rate, calculations of the thickness of any intermetallic layer grown from an undersaturated solder melt are carried out twice for each point,  $t$ , by putting in the denominator of Eq. 8 first equal to  $(b_0 + b_t)/2$  and then  $b_t$ . Underestimated,  $x_{\text{under}}$ , and overestimated,  $x_{\text{over}}$ , layer thicknesses are thus obtained. Clearly, experimental values,  $x_{\text{exp}}$ , must lie somewhere in between, as is indeed the case for the  $Fe_2Al_5$  [13] and  $NiBi_3$  [15] layers.

In the case of the saturated 87.5% Sn-7.5% Bi-3% In-1% Zn-1% Sb solder melt, the experimental value of the  $Ni_3Sn_4$  layer thickness (whenever it has not been destroyed under the influence of the liquid phase) was found to be  $16.0 \times 10^{-6} \text{ m}$  at 450 °C and a dipping time of 300 s.

Hence,  $k_1 = x^2/2t = 4.3 \times 10^{-13} \text{ m}^2 \text{ s}^{-1}$ . Other quantities necessary for calculations are  $k = 6.2 \times 10^{-5} \text{ m s}^{-1}$  at  $\omega = 24.0 \text{ rad s}^{-1}$ ,  $c_s = 48.5 \text{ kg m}^{-3}$  (0.69% Ni in the soldering alloy),  $\rho = 8.68 \times 10^3 \text{ kg m}^{-3}$  [19],  $\phi = 0.27$ ,  $s/v = 10.0 \text{ m}^{-1}$ ,  $b_0 = 1.28 \times 10^{-6} \text{ m s}^{-1}$ .

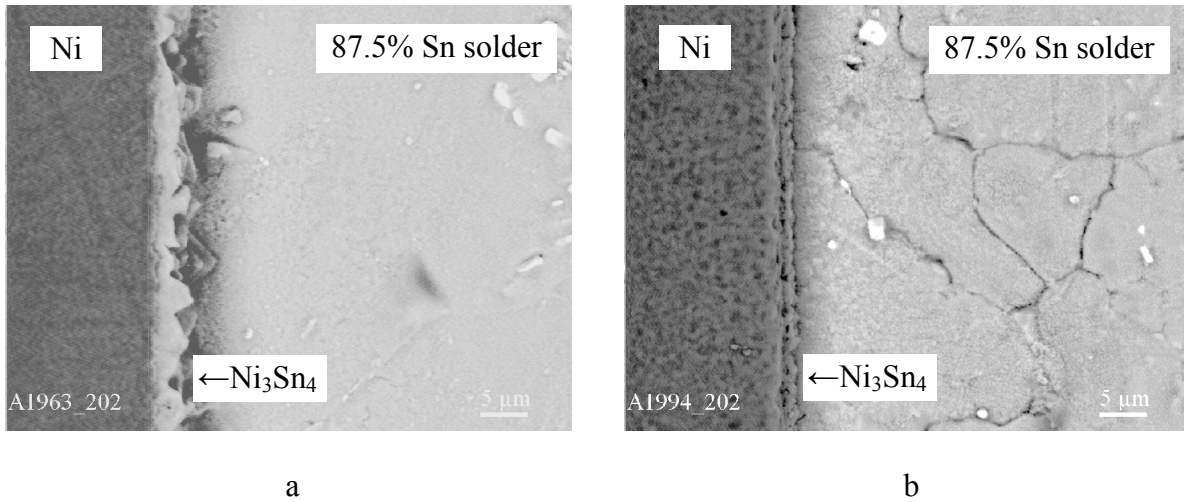


Figure 4 Backscattered electron image of the transition zone formed between nickel and a liquid 87.5% Sn-7.5% Bi-3% In-1% Zn-1% Sb soldering alloy at a temperature of 350 °C and a dipping time of 300 s. (a) saturated melt, (b) undersaturated melt ( $\omega = 24.0 \text{ rad s}^{-1}$ )

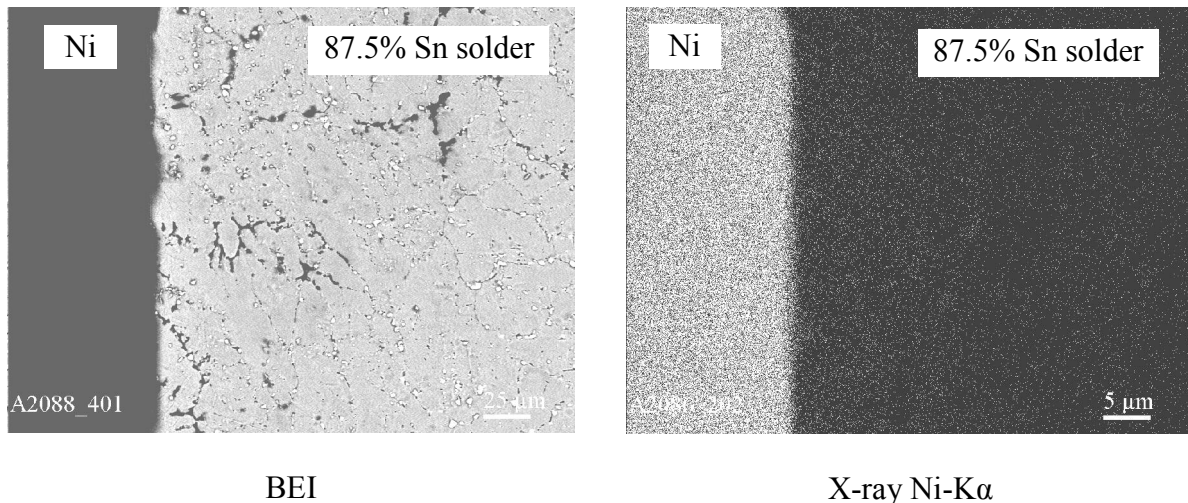


Figure 5 Backscattered electron image (BEI) and X-ray map of the transition zone between nickel and the undersaturated 87.5% Sn-7.5% Bi-3% In-1% Zn-1% Sb solder melt at a temperature of 250 °C, a dipping time of 600 s and a rotational speed of 24.0  $\text{rad s}^{-1}$

Using these data, one obtains the limiting values,  $x_{\text{under}} = 0.6 \times 10^{-6}$  m and  $x_{\text{over}} = 1.5 \times 10^{-6}$  m, for the thickness of the  $\text{Ni}_3\text{Sn}_4$  layer grown from the undersaturated solder melt at 450 °C and a dipping time of 2400 s. The experimental value,  $x_{\text{exp}}$ , is  $(1.2 \pm 0.2) \times 10^{-6}$  m. The agreement of these values appears to be quite sufficient for practical purposes to roughly estimate the intermetallic layer thickness at the solid metal-liquid solder interface.

### Tensile strength of nickel-to-solder joints

The nickel-to-solder transition joints were made by means of interaction of solid nickel specimens, 8 mm in diameter, with soldering alloy melts under strictly specified conditions of temperature, time and liquid agitation, followed by their joint cooling at a controlled rate until the melt crystallizes. Their uniaxial tensile tests were carried out on a P-500 tester. The gauge length of the Sn-alloy part was 8-12 mm, while the diameter was 5.9-6.8 mm. During the tensile tests, the crosshead speed was equal to  $0.1 \text{ mm s}^{-1}$ .

As seen in Fig. 6, the failure occurred in a brittle manner with a slight plastic deformation either along or 1-7 mm away from the interface between dissimilar materials. The rupture strength,  $\sigma$ , was found to be  $94 \pm 4$  MPa with a 87.5% Sn-7.5% Bi-3% In-1% Zn-1% Sb solder and  $102 \pm 5$  MPa with a 80% Sn-15% Bi-3% In-1% Zn-1% Sb solder. These values are more than two times greater than those (37-42 MPa [12]) for conventional Sn-Pb solders. The relative elongation was 2.0-2.5%.

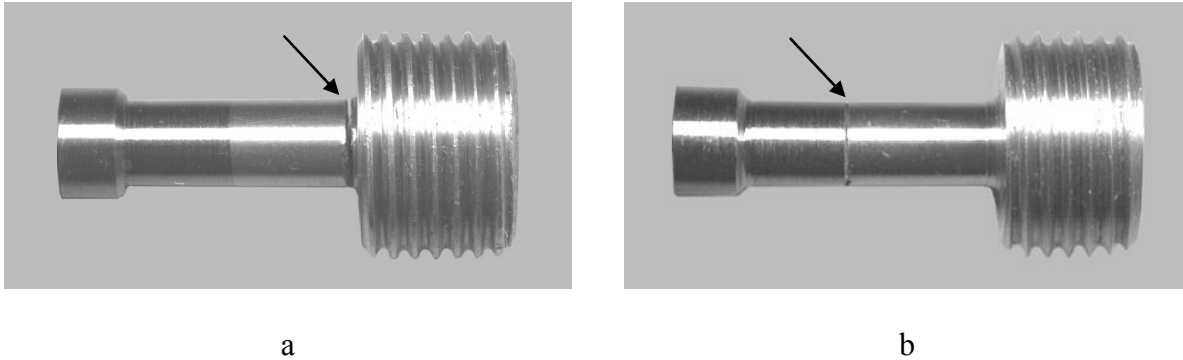


Figure 6 Transition joints of nickel with soldering alloys after tensile tests. The rupture place is indicated by an arrow.  
(a) 87.5% Sn-7.5% Bi-3% In-1% Zn-1% Sb solder, (b) 80% Sn-15% Bi-3% In-1% Zn-1% Sb solder

### Conclusions

The dissolution process of nickel in liquid 87.5% Sn-7.5% Bi-3% In-1% Zn-1% Sb and 80% Sn-15% Bi-3% In-1% Zn-1% Sb solders is characterized by two quantities: the solubility,  $c_s$ , and the dissolution rate constant,  $k$ . The temperature dependence of the solubility of nickel in those solders is described in the 250–450 °C range by an equation of the Arrhenius type  $c_s = A \exp(-E/RT)$ , where  $A = 4.94 \times 10^2$  % and  $E = 39.5 \text{ kJ mol}^{-1}$  for a 87.5% Sn-7.5% Bi-3% In-1%

Zn-1% Sb solder and  $A = 4.19 \times 10^2$  % and  $E = 40.2 \text{ kJ mol}^{-1}$  for a 80% Sn-15% Bi-3% In-1% Zn-1% Sb solder.

In spite of the great difference in solubility values, appropriate dissolution rate constants and diffusion coefficients of nickel are rather close for these solders.

With both solders, the single-phase  $\text{Ni}_3\text{Sn}_4$  intermetallic layer is formed at the interface of nickel and the saturated or undersaturated solder melt. In the case of undersaturated melts, the  $\text{Ni}_3\text{Sn}_4$  layer thickness can readily be evaluated using the proposed simple mathematical equations.

The tensile strength of the nickel-to-alloy transition joints is more than twice that of conventional Sn-Pb solders. The plasticity of cast Sn-Bi-In-Zn-Sb soldering alloys is rather low.

The data presented can be used in practice to evaluate (i) the thickness of the dissolved portion of the solid nickel material during soldering, (ii) the extent of saturation of a solder with nickel and (iii) the effect of dissolution on the growth rate of intermetallic layers at the Ni-solder interface.

### Acknowledgments

This investigation was supported in part by the US Civilian Research and Development Foundation grant No. UKE2-2698-KV-06. The authors thank L.A. Duma for taking X-ray patterns, L.M. Kuzmenko for carrying out chemical analyses, D.M. Pashko for machining nickel specimens and other mechanical work, E.S. Rabotina for making metallic cross-sections, and I.G. Kondratenko and S.V. Bykova for their help in conducting the experiments.

### References

- [1] M.S. Lee, C. Chen, and C.R. Kao, Formation and Absence of Intermetallic Compounds during Solid-State Reactions in the Ni-Bi system, *Chem. Mater.*, Vol 11, 1999, p. 292-297
- [2] W.H. Tao, C. Chen, C.E. Ho, W.T. Chen, and C.R. Kao, Selective Interfacial Reaction between Ni and Eutectic BiSn Lead-Free Solder, *Chem. Mater.*, Vol 13, 2001, p. 1051-1056
- [3] John N. Lalena, Nancy F. Dean, and Martin W. Weiser, Experimental Investigation of Ge-Doped Bi-11Ag as a New Pb-Free Solder Alloy for Power Die Attachment, *J. Electronic Mater.*, Vol 31, 2002, p. 1244-1249
- [4] M.Y. Chiu, S.S. Wang, T.H. Chuang, Intermetallic Compounds Formed during Interfacial Reactions between Liquid Sn-8Zn-3Bi Solders and Ni Substrates, *J. Electronic Mater.*, Vol 31, 2002, p. 494-499
- [5] M.O. Alam, Y.C. Chan, and K.N. Tu, Effect of Reaction Time and P Content on Mechanical Strength of the Interface Formed between Eutectic Sn-Ag Solder and Au/Electroless Ni(P)/Cu Bond Pad, *J. Appl. Phys.*, Vol 94, 2003, p. 4108-4115
- [6] Jeong-Won Yoon, Sang-Won Kim, Ja-Myeoung Koo, Dae-Gon Kim, and Seoung-Boo Jung, Reliability Investigation and Interfacial Reaction of Ball-Grid-Array Packages Using the Lead-Free Sn-Cu Solder, *J. Electronic Mater.* Vol 33, 2004, p. 1190-1199
- [7] Hwa-Teng Lee, Heng-Sheng Lin, Cheng-Shyan Lee, and Po-Wei Chen, Reliability of Sn-Ag-Sb Lead-Free Solder Joints, *Mater. Sci. Eng. A*, Vol 407, 2005, p. 36-44
- [8] P.L. Liu and J.K. Shang, Segregant-Induced Cavitation of Sn-Cu Reactive Interface, *Scripta Mater.*, Vol 53, 2005, p. 631-634

- [9] M.J. Rizvi, Y.C. Chan, C. Bailey, H. Lu, and M.N. Islam, Effect of Adding 1 wt% Bi into the Sn-2.8Ag-0.5Cu Solder Alloy on the Intermetallic Formations with Cu-Substrate during Soldering and Isothermal Aging, *J. Alloys Comp.*, Vol 407, 2006, p. 208-214
- [10] Chao-hong Wang, Sinn-wen Chen, Sn-0.7 wt.% Cu/Ni Interfacial Reactions at 250 °C, *Acta Mater.*, Vol 54, 2006, p. 247253.
- [11] M. Hansen, *Constitution of binary alloys*, McGraw-Hill, New-York, 1958
- [12] S.V. Lashko and N.F. Lashko, *Paika metallov*, Mashinostroenie, Moskwa, 1988
- [13] K. Barmak and V.I. Dybkov, Interaction of Iron-Chromium Alloys Containing 10 and 25 Mass% Chromium with Liquid Aluminium, *J. Mater. Sci.*, Vol 39, 2004, p. 4219-4230
- [14] G.A. Pribytkov and V.I. Itin, Kinetika Rastvoreniya Nikelya i Stannidov Nikelya v Zhidkom Olove, *Izv. Vuzov: Fizika*, Vol 9, 1975, p. 100-105
- [15] V.I. Dybkov, K. Barmak, W. Lengauer, and P. Gas, Interfacial Interaction of Solid Nickel with Liquid Bismuth and Bi-Base Alloys, *J. Alloys Comp.*, Vol 389, 2005, p. 61-74
- [16] V.G. Levich, *Fiziko-Khimicheskaya Hidrodinamika*, Fizmatgiz, Moskwa, 1959
- [17] T.F. Kassner, Rate of Solution of Rotating Ta Disks in Liquid Tin, *J. Electrochem. Soc.*, Vol 114, 1967, p. 689-694
- [18] V.I. Dybkov, *Reaction Diffusion and Solid State Chemical Kinetics*, The IPMS Publications, Kyiv, 2002; free access <http://users.i.com.ua/~dybkov/V/>
- [19] H.J. Wallbaum, Uber intermetallische Germaniumverbindungen, *Naturwissenschaften*, Vol 32, 1944, p. 76